University of California
Los Angeles

Numerical Studies of Turbulence in LAPD

A dissertation submitted in partial satisfaction
of the requirements for the degree
Doctor of Philosophy in Physics

by

Brett Cory Friedman

2012

Abstract of the Dissertation

Numerical Studies of Turbulence in LAPD

by

Brett Cory Friedman

Doctor of Philosophy in Physics

University of California, Los Angeles, 2012

Professor Troy A. Carter, Chair

To be completed

The dissertation of Brett Cory Friedman is approved.

Warren B. Mori

George J. Morales

Russel E. Caflisch

Troy A. Carter, Committee Chair

University of California, Los Angeles

2012

To be completed . . .

Table of Contents

List of Figures

List of Tables

Acknowledgments

To be completed ...

Vita

2003-2007	Regent Scholar, University of California, Irvine.
2007	B.S. (Physics) Summa Cum Laude, University of California, Irvine.
2007	Chancellor's Fellow, University of California, Los Angeles.
2007-2009	Teaching Assistant, Department of Physics and Astronomy, University of California, Los Angeles.
2009-2013	Research Assistant, Department of Physics and Astronomy, University of California, Los Angeles.
2009-2012	ORISE FES Fellow, University of California, Los Angeles.
2012-2013	Dissertation Year Fellow, University of California, Los Angeles.

Publications

B. Friedman, T. A. Carter, M. V. Umansky, D. Schaffner, and B. Dudson, Energy dynamics in a simulation of LAPD turbulence, Phys. Plasmas, 102307 (2012).

D. A. Schaffner, T. A Carter, G. D. Rossi, D. S. Guice, J. E. Maggs, S. Vincena, and B. Friedman, Modification of Turbulent Transport with Continuous Variation of Flow Shear in the Large Plasma Device, Phys. Rev. Lett. 109, 135002 (2012).

S. Zhou, W. W. Heidbrink, H. Boehmer, R. McWilliams, T. A. Carter, S. Vincena, B. Friedman, and D. Schaffner, Sheared-flow induced confinement transition in a linear magnetized plasma, Phys. Plasmas 19, 012116 (2012).

B. Friedman, M. V. Umansky, and T. A. Carter, Grid convergence study in a simulation of LAPD turbulence, Contrib. Plasma Phys. 52, 412 (2012).

M. V. Umansky, P. Popovich, T. A. Carter, B. Friedman, and W. M. Nevins, Numerical simulation and analysis of plasma turbulence the Large Plasma Device, Phys. Plasmas 18, 055709 (2011).

P. Popovich, M.V. Umansky, T.A. Carter, and B. Friedman, Modeling plasma turbulence and transport in the Large Plasma Device, Phys. Plasmas 17, 122312 (2010).

P. Popovich, M.V. Umansky, T.A. Carter, and B. Friedman, Analysis of plasma instabilities and verification of the BOUT code for the Large Plasma Device, Phys. Plasmas 17, 102107 (2010).

S. Zhou, W. W. Heidbrink, H. Boehmer, R. McWilliams, T. A. Carter, S. Vincena, S. K. P. Tripathi, P. Popovich, B. Friedman, and F. Jenko, Turbulent transport of fast ions in the Large Plasma Device, Phys. Plasmas 17, 092103 (2010).

B. Friedman, M. V. Umansky, and T. A. Carter, Grid convergence study in a simulation of LAPD turbulence, Contrib. Plasma Phys. 52, 412 (2012).

CHAPTER 1

Introduction

CHAPTER 2

Turbulence and Instability

2.1 The Kolmogorov Paradigm of Turbulence

2.2 The Standard Plasma Paradigm of Linear Instability

2.3 Nonlinear Stability Effects

2.4 Nonlinear Stability Effects in Plasma Physics

CHAPTER 3

The Braginskii Fluid Model and LAPD

3.1 LAPD Suitability to the Braginskii Fluid Model

At a basic level, the state of a plasma is described by seven-dimensional distribution functions $f_j(\mathbf{x}, \mathbf{v}, t)$ for each species j. The behavior of the plasma is described by the system of kinetic equations (Boltzmann equations), which evolve the distribution functions forward in time:

$$\frac{\partial f_j}{\partial t} + \mathbf{v} \cdot \nabla f_j + \frac{e_j}{m_j}(\mathbf{E} + \mathbf{v} \times \mathbf{B}) \cdot \frac{\partial f_j}{\partial \mathbf{v}} = \left(\frac{\partial f_j}{\partial t}\right)_C . \tag{3.1}$$

$\left(\frac{\partial f_j}{\partial t}\right)_C$ is the change in the distribution function due to collisions. For plasmas, the collisions are Coulomb collisions, and the collision term takes the form of the Fokker-Planck operator. With this operator, Eq. 3.1 is called the Fokker-Planck equation. Now it is well known that the Fokker-Planck equation cannot be solved numerically for problems that require time intervals much larger than the electron-cyclotron time due to computational and time limitations. The phase space is just too large. Therefore, reduced equations, such as gyrokinetic, drift kinetic, or fluid equations have been derived to produce numerically tractable equations. These equations are all derived under certain physical assumptions such as strong guiding magnetic fields, small fluctuation levels, or slow spatial and/or time variations such that these different equations are best applied to different physical situations.

The equations that are arguably most suitable to describe waves and turbulence in LAPD (and fastest to solve numerically) are the fluid equations, specif-

ically those derived by Braginskii [Bra65]. In deriving his equations, Braginskii approximates the solution as $f_j = f_j^0 + f_j^1$ where the zero-order piece f_j^0 is a Maxwellian and the first-order piece f_j^1 is a perturbation on the zero-order distribution function: $|f_j^1| \ll f_j^0$. The equations are then derived by taking moments of the Fokker-Planck equation to create coupled equations of the independent variables, $n_j, \mathbf{v_j}$, and T_j. Now certain requirements must hold to justify the Braginskii approximation, all of which have the flavor that macroscopic quantities must vary slowly in time and space. This is generally caused by strong relaxation processes such as collisions, which keep the distribution functions close to Maxwellians. In general, for the Braginskii equations to be applicable, processes of interest must occur on time intervals much greater than the collision time and quantities should vary slowly over distances traversed by the particles between collisions.

Specifically, the requirement that time variations must be slow can be written $\frac{d}{dt} \ll \nu$, where for electron drift wave turbulence, this is approximately $\omega_* \ll \nu_e$. Table 4.5, which displays typical LAPD operating parameters, shows that $\omega_*/\nu_e \sim 0.01$. The requirement that spatial quantities vary slowly compared to the collisional mean free path can be written simply for the direction parallel to the magnetic field as $\lambda_{ei} \sim \lambda_{ee} \ll L_\parallel$. For LAPD, $\lambda_{ei}/L_\parallel \sim 0.01$. For the direction perpendicular to the magnetic field, the same kind of relation $\lambda_{mfp} \ll L_\perp$ must also hold. However, due to the cyclotron motion of particles around the magnetic field, λ_{mfp} is really the larmor radius, unless the collisional mean free path is less than the larmor radius. For electrons, $\rho_e \ll \lambda_{ei}$ and $\rho_e/L_\perp \sim 10^{-4}$ where $L_\perp \sim 0.1$ m. For the ions, the ion cyclotron frequency is close to the ion collision frequency, meaning that either the ion larmor radius or the ion mean free path may be used. Using the larmor radius, $\rho_i/L_\perp \sim 0.01$. Therefore, the collisionality is high enough and the machine dimensions are large enough so that the Braginskii fluid model should be applicable to LAPD.

3.2 The Braginskii Equations

The Braginskii fluid equations are as follows: the continuity equation for species j, electrons or ions, is [Wes04, Bra65]

$$\frac{\partial n_j}{\partial t} = -\nabla \cdot (n_j \mathbf{v}_j). \tag{3.2}$$

The momentum balance equation is

$$n_j m_j \frac{d\mathbf{v}_j}{dt} = -\nabla p_j - \frac{\partial \Pi_{j\alpha\beta}}{\partial x_\beta} + n_j e_j(\mathbf{E} + \mathbf{v_j} \times \mathbf{B}) + \mathbf{R}_j. \tag{3.3}$$

$p_j = n_j T_j$ is the pressure. $\Pi_{j\alpha\beta}$ is the stress tensor, which involves the products of viscosity coefficients and rate-of-strain tensor components. The viscosity coefficients are some of the several terms that are called transport coefficients. The transport coefficients are calculated by the Braginskii procedure in terms of n, $\mathbf{v}$, and T. $\mathbf{R}_j$, which involves several other transport coefficients, is the rate of collional momentum transfer. The momentum transfer from ions to electrons is given by

$$\mathbf{R}_e = -m_e n_e \nu_e (0.51 u_{\parallel e} + \mathbf{u}_{\perp e}) - 0.71 n_e \nabla_\parallel T_e - \frac{3}{2}\frac{n_e \nu_e}{\omega_{ce}} \mathbf{b} \times \nabla T_e \tag{3.4}$$

where $\mathbf{u} = \mathbf{v}_e - \mathbf{v}_i$ and ν_e is the electron collision frequency with ions. $\mathbf{R}_e$ includes both the friction force and the thermal force, which, like the friction force, is due to electron-ion collisions, but originates from the temperature dependence of the collisionality. The thermal force terms are those proportional to the gradients of temperature. $\mathbf{R}_i = -\mathbf{R}_e$ in a fully ionized plasma with one ion species. However, LAPD has a significant neutral density. Collisions with neutrals are much more important for the ions [PUC10]. So

$$\mathbf{R}_i = -\mathbf{R}_e - n_i m_i \nu_{in} \mathbf{v_i}. \tag{3.5}$$

The energy balance equation is

$$\frac{3}{2}n_j\frac{\partial T_j}{\partial t} = -n\mathbf{v}_j\cdot\nabla T_j - p_j\nabla\cdot\mathbf{v}_j - \nabla\cdot\mathbf{q}_j - \Pi_{j\alpha\beta}\frac{\partial v_j\alpha}{\partial x_\beta} + Q_j \tag{3.6}$$

where the term involving the stress tensor describes viscous heating. The electron heat flux (with more transport coefficients) is

$$q_e = n_eT_e\left(0.71u_\parallel + \frac{3\nu_e}{2\omega_{ce}}\mathbf{b}\times\mathbf{u}\right) + \frac{n_eT_e}{m_e\nu_e}\left(-3.16\nabla_\parallel T_e - \frac{4.66\nu_e^2}{\omega_{ce}^2}\nabla_\perp T_e - \frac{5\nu_e}{2\omega_{ce}}\mathbf{b}\times\nabla T_e\right) \tag{3.7}$$

where the first part of this expression constitutes convection, while the second part is conduction. The ion heat flux is

$$q_i = \frac{n_iT_i}{m_i\nu_i}\left(-3.9\nabla_\parallel T_i - \frac{2\nu_i^2}{\omega_{ci}^2}\nabla_\perp T_i - \frac{5\nu_i}{2\omega_{ci}}\mathbf{b}\times\nabla T_i\right). \tag{3.8}$$

The last transport coefficients are in the heating Q. The ion heating due to collisional heat exchange between ions and electrons is

$$Q_i = \frac{3m_e}{m_i}n_e\nu_e(T_e - T_i) \tag{3.9}$$

while the electron heating is

$$Q_e = -\mathbf{R}\cdot\mathbf{u} - Q_i. \tag{3.10}$$

The electron heat exchange involves an ohmic heating contribution ($\mathbf{R}\cdot\mathbf{u}$) that is absent from the ion heating because electrons colliding with ions transfer very little momentum to the ions.

3.3 The Vorticity Equation

Now the Braginskii equations in the previous section contain electric and magnetic fields which must be self-consistently determined by the charges and currents that are evolved by the equations. This is done with the inclusion of Maxwell's equations. Two of those equations are used to write the fields in terms of potentials:

$$\begin{aligned} \mathbf{E} &= -\nabla\phi - \frac{\partial \mathbf{A}}{\partial t} \\ \mathbf{B} &= \nabla \times \mathbf{A}. \end{aligned} \tag{3.11}$$

The vector potential $\mathbf{A}$ is strictly a fluctuating quantity, meaning it is not used to describe the guide field $\mathbf{B}_0$. The next equation,

$$\nabla \times \mathbf{B} = \nabla(\nabla \cdot \mathbf{A}) - \nabla^2 \mathbf{A} = \mu_0 \mathbf{j} \tag{3.12}$$

is used to relate the vector potential to the current, where the displacement current is neglected as is generally done in plasmas. The Poisson equation is not that useful for the main part of the plasma, in which the quasineutrality relation, $n_e = n_i \equiv n$, holds. The useful equation that can be used instead is the conservation of charge (or ambipolarity condition), $\nabla \cdot \mathbf{j} = 0$. The vorticity equation is derived from this conservation of charge equation.

The current is $\mathbf{j} = en(v_{\parallel i} - v_{\parallel e}) + en(\mathbf{v}_{\perp i} - \mathbf{v}_{\perp e})$. In LAPD, the parallel current is carried primarily by the fast streaming electrons, while the perpendicular current is primarily carried by the ions, which have larger Larmor radii. So the conservation of charge equation can be simplified to

$$\nabla_\parallel (n v_{\parallel e}) = \nabla_\perp \cdot (n \mathbf{v}_{\perp i}). \tag{3.13}$$

The perpendicular ion component of this equation is derived from Eq. 3.3

for the ions. Neglecting terms that have finite ion temperature (pressure and stress tensor), and solving for the ion velocity in the Lorentz force term, the perpendicular ion velocity has three terms [PUC10, SC03]:

$$\mathbf{v}_{\perp i} = \mathbf{v}_E + \mathbf{v}_{pi} + \mathbf{v}_{\nu i} \tag{3.14}$$

where the $\mathbf{E} \times \mathbf{B}$ velocity is $\mathbf{v}_E = \mathbf{E} \times \mathbf{B}/B^2 = -\nabla_\perp \phi \times \mathbf{B}/B^2$, the polarization velocity is $\mathbf{v}_{pi} = (1/\omega_{ci})\mathbf{b} \times (\partial_t + \mathbf{v}_i \cdot \nabla)\mathbf{v}_i$, and the Pedersen velocity is $\mathbf{v}_{\nu i} = (\nu_{in}/\omega_{ci})\mathbf{b} \times \mathbf{v}_i$. The charge conservation equation then takes the form:

$$\nabla_\parallel (n v_{\parallel e}) = \frac{1}{\omega_{ci}} \nabla_\perp \cdot \left[n\mathbf{b} \times (\partial_t + \mathbf{v}_i \cdot \nabla + \nu_{in})\mathbf{v}_i \right]. \tag{3.15}$$

Note that the $\mathbf{E} \times \mathbf{B}$ velocity doesn't contribute to the current due to the electrons producing an equal and opposite $\mathbf{E} \times \mathbf{B}$ current. We now employ the approximation $\mathbf{v}_i \sim \mathbf{v}_E$ to Eq. 3.15. This approximation wasn't appropriate of course for Eq. 3.14 due to the fact that $\mathbf{v}_E$ doesn't contribute to the current, but it is appropriate here. Then,

$$\begin{aligned} \nabla_\parallel (n v_{\parallel e}) &= \frac{1}{\omega_{ci}} \nabla_\perp \cdot \left[n\mathbf{b} \times (\partial_t + \mathbf{v}_E \cdot \nabla + \nu_{in})\mathbf{v}_E \right] \rightarrow \\ \nabla_\parallel (n v_{\parallel e}) &= -\frac{m_i}{eB^2} \nabla_\perp \cdot \left[n\mathbf{b} \times (\partial_t + \mathbf{v}_E \cdot \nabla + \nu_{in})\nabla_\perp \phi \right]. \end{aligned} \tag{3.16}$$

Next, defining the vorticity as $\varpi \equiv \nabla_\perp \cdot (n \nabla_\perp \phi)$, the vorticity equation reads,

$$\frac{\partial \varpi}{\partial t} = -\mathbf{v}_E \cdot \nabla_\perp \varpi - \nabla_\perp \mathbf{v}_E : \nabla_\perp (n \nabla_\perp \phi) - \frac{eB^2}{m_i} \nabla_\parallel (n v_{\parallel e}) - \nu_{in} \varpi. \tag{3.17}$$

Finally, the term with the tensor product can be rewritten in a different form [PUC10]:

$$\frac{\partial \varpi}{\partial t} = -\mathbf{v}_E \cdot \nabla_\perp \varpi + \frac{1}{2}(\mathbf{b} \times \nabla_\perp n) \cdot \nabla_\perp \mathbf{v}_E^2 - \frac{eB^2}{m_i} \nabla_\parallel (n v_{\parallel e}) - \nu_{in} \varpi. \tag{3.18}$$

3.4 Minimizing the Equation Set for LAPD Parameters

3.4.1 The Reduced Equations

The continuity equations 3.2 for electrons and ions do not have to both be used due to the quasineutrality condition $n_e = n_i \equiv n$. So, if one focuses on the electron continuity equation, then,

$$\frac{\partial n}{\partial t} = -\nabla \cdot (n\mathbf{v}_e). \tag{3.19}$$

Now, $\mathbf{v}_e = \mathbf{v}_{\perp e} + v_{\parallel e}$, where $\mathbf{v}_{\perp e} = \mathbf{v}_E + \mathbf{v}_{de} + \mathbf{v}_{pe}$, with the diamagnetic velocity $\mathbf{v}_{de} = -\frac{\mathbf{b}\times\nabla p_e}{en_eB}$, which wasn't included for the ions in Eq. 3.14 due to the neglect of ion pressure. To a good approximation, $\nabla \cdot (n\mathbf{v}_{\perp e}) = \mathbf{v}_E \cdot \nabla n$ [PUC10, SC03]. So, the continuity equation reads

$$\frac{\partial n}{\partial t} = -\mathbf{v}_E \cdot \nabla n - \nabla_\parallel (n v_{\parallel e}). \tag{3.20}$$

Next, the momentum equations (Eq. 3.3), of which there are six (three for electron velocity components and three for ion velocity components) are reduced to two here. The first is the vorticity equation (Eq. 3.18), in which we used the perpendicular momentum equations to derive it. The second is the equation for the parallel electron momentum. We neglect the parallel ion momentum equation since $v_{\parallel e} \gg v_{\parallel i}$ for LAPD. The electron parallel momentum equation is then

$$nm_e \frac{\partial v_{\parallel e}}{\partial t} = -nm_e \mathbf{v}_E \cdot \nabla v_{\parallel e} - \nabla_\parallel p_e - enE_\parallel - 0.71 n \nabla_\parallel T_e - 0.51 m_e n \nu_e v_{\parallel e}, \tag{3.21}$$

where the viscous terms have been neglected. The conservation of energy equations (Eq. 3.6) are left. Since the ion temperature in LAPD is very low ($T_i \leq 1$ eV), the ion energy equation is neglected. The electron energy equation is [SC03]

$$\frac{3}{2}n\frac{\partial T_e}{\partial t} = -\frac{3}{2}n\mathbf{v}_E \cdot \nabla T_e - p_e \nabla_\parallel v_{\parallel e} \tag{3.22}$$
$$+0.71 T_e \nabla \cdot (n v_{\parallel e}) + \nabla_\parallel (\kappa_{\parallel e} \nabla_\parallel T_e) + 0.51 m_e n \nu_e v_{\parallel e}^2 - 3\frac{m_e}{m_i} n \nu_e T_e,$$

where $\kappa_{\parallel e} = 3.16 \frac{n T_e}{m_e \nu_e}$.

3.4.2 The Electrostatic Justification

Plasma currents create magnetic fields in plasmas. Often times, analytic and numerical calculations of plasma waves and turbulence neglect the time dependent magnetic field perturbations, focusing only on the electrostatic contribution to the waves, turbulence, and transport. In the reduced fluid equations of the previous subsection, the magnetic perturbation enters in two important ways. First, it enters the electric field term of Eq. 3.21 because $E_\parallel = -\nabla_\parallel \phi - \frac{\partial A_\parallel}{\partial t}$, where $A_\parallel$ is the parallel component of the vector potential. Second, it affects the parallel gradient operator, $\nabla_\parallel = \mathbf{b} \cdot \nabla$ where $\mathbf{b}$ is in the direction of the total magnetic field [SC03]. In the electrostatic limit, $A_\parallel \to 0$, so $E_\parallel = -\nabla_\parallel \phi$ and $\nabla_\parallel = \mathbf{b}_0 \cdot \nabla$. We take this limit in the remaining chapters, but there is the question of how justified we are to do so.

As a first step in answering this question, examine Eq. 3.21. The four independent variables, $n, \phi, v_{\parallel e}$, and T_e, which each have their own evolution equation, are all present in Eq. 3.21. Taking the parallel projection of Eq. 3.12 gives

$$\nabla_\perp^2 A_\parallel = -\mu_0 j_\parallel = \mu_0 n e v_{\parallel e}. \tag{3.23}$$

So $A_\parallel \sim \mu_0 n e L_\perp^2 v_{\parallel e}$, where $\nabla_\perp^2 \sim 1/L_\perp^2$. Then, Eq. 3.21 can be approximately rewritten as,

$$n m_e \frac{dv_{\parallel e}}{dt} \sim -T_e \nabla_\parallel n + e n \nabla_\parallel \phi + \mu_0 e^2 n^2 L_\perp^2 \frac{\partial v_{\parallel e}}{\partial t} - 1.71 n \nabla_\parallel T_e - 0.51 m_e n \nu_e v_{\parallel e}. \tag{3.24}$$

The electromagnetic induction term, ($EM = en\frac{\partial A_\parallel}{\partial t}$) is now written in terms of $v_{\parallel e}$ as $EM = \mu_0 e^2 n^2 L_\perp^2 \frac{\partial v_{\parallel e}}{\partial t}$. It can therefore be directly compared to the other terms proportional to $v_{\parallel e}$ to test for its importance. The other terms are the inertial term, $M = nm_e\frac{dv_{\parallel e}}{dt}$ and the resistive term, $R = 0.51 m_e n \nu_e v_{\parallel e}$. A common way to compare these terms is to approximate the time derivative as the ion cyclotron frequency $\frac{\partial}{\partial t} \sim \omega_{ci}$ and the perpendicular length scale as the ion sound gyroradius $L_\perp \sim \rho_s$, where $\rho_s = c_s/\omega_{ci}$. Then the ratio of the three terms (obtained by dividing each term by $eBnv_{\parallel e}$) is:

$$M : EM : R = \frac{m_e}{m_i} : \beta : \frac{0.51\nu_e}{\omega_{ce}}. \tag{3.25}$$

It can be seen from Table 4.5 that in LAPD, this ratio is $1 : 3.6 : 1.5$. Thus, all three terms are of the same order with the electromagnetic term slightly larger than the other two. It seems then quite unjustified to use an electrostatic approximation.

However, estimating $\frac{\partial}{\partial t} \sim \omega_{ci}$ isn't necessarily accurate. The equation set describes drift waves and so a more proper estimate might be $\frac{\partial}{\partial t} \sim \omega_*$. Under this approximations, the ratio is $1 : 3.6 : 70$, meaning that the resistive term is more than an order of magnitude larger than the other two; however, the approximation $\frac{\partial}{\partial t} \sim \omega_*$ is still rough and the numerical value of ω_* in Table 4.5 is somewhat of a rough itself. Moreover, one could also argue with the approximation of the perpendicular length scale as the sound gyroradius. This is probably too small, in which case the electromagnetic inductance has been underestimated. While it's clear that the inertial term is probably unimportant, the inductive term could be important.

Similarly, the contribution of $\tilde{\mathbf{b}} \sim A_\parallel$ in $\nabla_\parallel$ can be approximated in a similar manner with similar inconclusive results. Without a clear separation between the resistive and inductive terms, the best way to determine the validity of the

electrostatic approximation is by direct numerical calculation of the turbulence with and without the electromagnetic contributions. Therefore, we simulated an electrostatic and two electromagnetic versions of LAPD turbulence. The details of the electrostatic code are described in Chapter 4 and in Appendix A.

The only difference between the electrostatic and the first electromagnetic simulation is the exclusion/inclusion of the electromagnetic term $en\frac{\partial A_\parallel}{\partial t}$ in the parallel electron momentum equation (Eq. 3.21). Of course the Maxwell equation (Eq. 3.12) must also be included for the electromagnetic simulation. The second electromagnetic simulation includes not only this term but also the $A_\parallel$ contribution to $\nabla_\parallel$ in the parallel electron momentum equation.

Now, turbulence is best characterized and compared in a statistical and often spectral manner. More details of turbulence characterization and comparison will be discussed later, but for now, we make a few statistical comparisons between the electrostatic and electromagnetic simulation results. Figure 3.1 shows the results of the three simulations as well as the experiment – namely, a comparison of the frequency spectra, the probability distribution function (pdf), and the rms level of the density fluctuations. Clearly, the fluctuations are statistically similar in all cases and none of the simulations are inconsistent with the experiment. However, the electromagnetic effects are noticable, and as we include more electromagnetic contributions in the simulations, the turbulent statistics more closely resemble those of the experiment. We make no quantitative comparison here, but rely only on a visual examination in making this conclusion.

Now, as mentioned above, we do not include any electromagnetic contributions in the simulations used in the following chapters. It seems rather unjustified to do so since we are clearly able to run electromagnetic simulations and they seem to reproduce experimental turbulence with slightly better accuracy than the electrostatic ones. One justification for our abandonment of electromagnetic simulations, however, is that electromagnetic simulations take a bit longer than

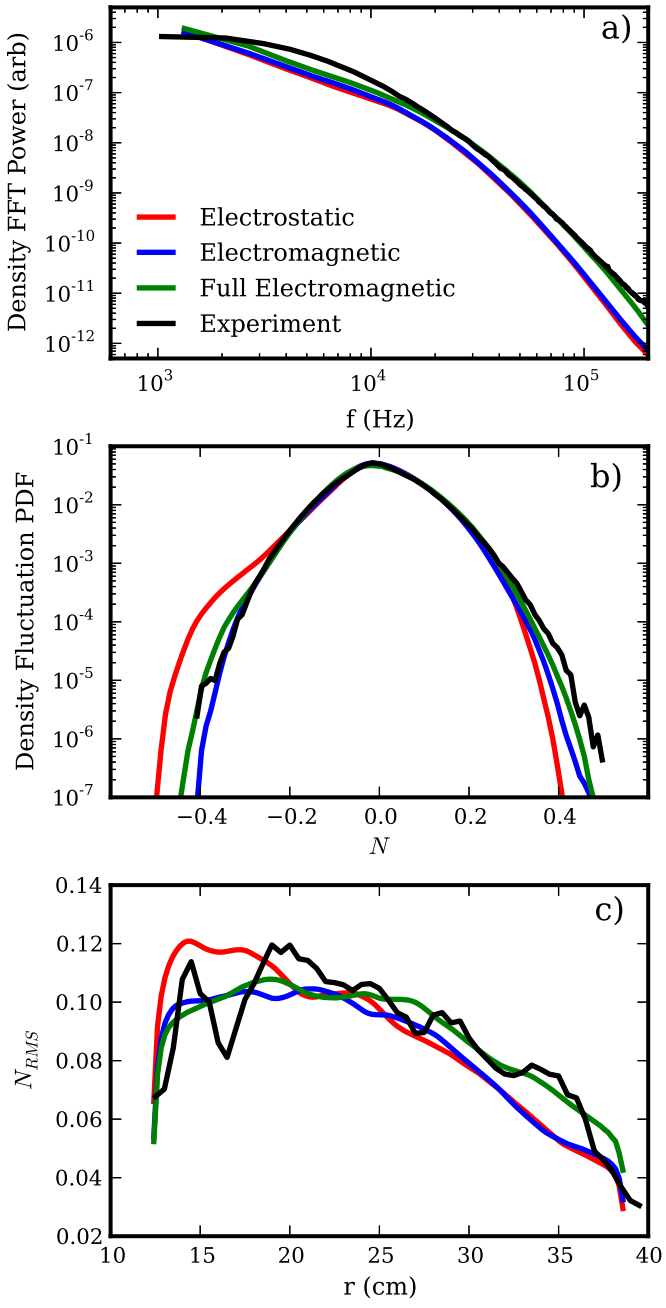

Figure 3.1: Statistical turbulent comparisons. The "Full Electromagnetic" curves are from the simulation including the $A_\parallel$ contribution to $\nabla_\parallel$, while the "Electromagnetic" curves just include the $A_\parallel$ contribution to $E_\parallel$.

electrostatic ones due to the extra relation in Eq. 3.12 that is used to solve for $A_\parallel$, which requires an inversion of the Laplacian. This takes extra computation. Another justification is that the electromagnetic equations make the energy dynamics analysis in Chapter 7 a bit more complicated. Both of these factors are mitigated, however, if the inertial term $nm_e\frac{dv_{\parallel e}}{dt}$ is dropped. Nevertheless, at the beginning of this work, we strived to find the simplest possible model to describe the turbulence in LAPD, and we determined that the electrostatic approximation was acceptable. At that time, we didn't have the results of Fig. 3.1. If we had the time, we would redo all of the simulations and analysis to include electromagnetic contributions, but drop the inertial term in Eq. 3.21. This is a clear route to take for future work. Nevertheless, we are confident that electromagnetics would not change any of our conclusions in this work. So for the remainder of this work, we will present theoretical calculations, simulation results, and conclusions using the electrostatic approximation.

CHAPTER 4

LAPD Simulation Details

4.1 The Equations

4.2 Finite Difference Schemes

4.3 Sources

4.4 Boundary Conditions

4.5 Profiles and Parameters

Species	^{4}He
Z	1
n	2.5×10^{18} m^{-3}
T_e	5 eV
T_i	$\lesssim 1$ eV
B_0	0.1 T
$L_\parallel$	17 m
a	0.4 m
λ_D	10^{-5} m
ω_{ci}	2.4×10^6 rad/s
ω_{ce}	1.8×10^{10} rad/s
ρ_e	5.3×10^{-5} m
ρ_i	$\sim 1 \times 10^{-3}$ m
ρ_s	5×10^{-3} m
v_{te}	9.4×10^5 m/s
c_s	1.1×10^4 m/s
v_A	7×10^5 m/s
β	5×10^{-4}
m_e/m_i	1.4×10^{-4}
$\ln\Lambda$	11
ν_e	7.2×10^6 Hz
λ_{ei}	0.13 m
ν_i	$\sim 10^6$ Hz
ν_{in}	1.2×10^3 Hz
$\kappa_\parallel^e$	9.8×10^{23} eV/m^2 s
η_0^i	$\sim 10^{12}$ eV s/m^3
ω_*	$\sim 5 \times 10^4$ rad/s

Table 4.1: Typical LAPD parameters

CHAPTER 5

Linear Instabilities

5.1 Drift Waves

5.2 Conducting Wall Mode

In this section, we consider the linear instability caused by a plasma bounded by two conducting walls on the boundaries where the magnetic field lines terminate (the axial boundaries). The instability is dependent upon Bohm sheath boundary conditions described in the following subsection. A point to note is that these boundary conditions are not necessarily the correct ones for LAPD. In tokamaks, the scrape-off-layer (SOL) can be characterized by a number of different regimes such as the sheath-limited, conduction-limited, or detached divertor regimes [Sta00]. The primary factor that controls which regime the SOL is in is the dimensionless collisionality $\nu^* \sim L/\lambda$ where L is the SOL length and λ is the electron or ion collision length. For LAPD, $\nu^* \sim 100$, which would put it in the detached regime. The Bohm sheath boundary condition is derived for low collisionality (the sheath-limited regime), so LAPD probably does not contain such a boundary condition. Yet, it is still academically instructive to apply such a boundary condition to LAPD because it creates a new linear instability, which can be used to test the robustness of LAPD's nonlinear instability.

5.2.1 The Bohm Sheath Boundary Condition

It is known that to good approximation, a plasma bounded by a wall can be divided into two regions: the main plasma and the Debye sheath [Sta00]. The Debye sheath is a small region adjacent to the wall, generally several Debye lengths long. It has a net positive charge ($n_i > n_e$) that shields the negative charge on the wall and serves to deflect some of the electrons that flow into the sheath. The sheath does not completely shield the negative wall, however, and a small electric field penetrates into the main plasma (the ambipolar field), which mostly serves to accelerate the cold ions toward the wall, and slightly retard the electrons before entering the sheath. In the main plasma, the quasineutrality relation holds ($n_i = n_e$).

The well-known Bohm criterion along with other considerations restricts the ions to move into the sheath entrance at the sound speed $c_s = \sqrt{T_e/m_i}$. We consider here the case where there is no external biasing; in other words, the end plates are electrically isolated and floating. The wall can be set to an arbitrary potential, say $\phi_w = 0$, while the potential at the sheath entrance is then the positive floating potential ϕ_{sf}. This potential difference across the sheath reflects slow electrons that enter the sheath. The electrons approximately maintain a cutoff Maxwellian velocity distrubution throughout the sheath, and at the wall, their velocity is retarded by a Boltzmann factor due to the floating potential. In total, the current to the wall is [BCR93]

$$J_{\parallel} = en\left[c_s - \frac{(T_e/m_e)^{1/2}}{2\sqrt{\pi}} exp^{(-\frac{e\phi_{sf}}{T_e})}\right]. \tag{5.1}$$

Note that this is not only the current to the wall, but also the current going into the sheath edge, as long as current isn't escaping radially and there isn't an ionization source within the sheath. Furthermore, since the wall is electrically isolated, the equilibrium current at the wall vanishes. This sets the value for the

floating potential to be $\phi_{sf} = \Lambda T_e/e$ with $\Lambda = ln(\frac{1}{2\sqrt{\pi}}\sqrt{\frac{m_i}{m_e}})$. Note that T_e is a function of radius, necessitating that ϕ_{sf} is also a function of radius. Thus, a radial equilibrium temperature gradient produces a radial equilibrium electric field. It is noted that $J_\parallel$ need not vanish on every field line since the end plates are conducting and charges can move around on the plate, however, the vanishing equilibrium current is generally a fair approximation [BCR93].

On the other hand, the fluctuating component of the current is allowed to vary between field lines. The first order fluctuating component is obtained by linearizing Eq. 5.1, giving the result:

$$\tilde{J}_\parallel = eN_0c_{s0}\left[\frac{e\tilde{\phi}}{T_{e0}} - \Lambda\frac{\tilde{T}_e}{T_{e0}}\right]. \tag{5.2}$$

This expression for the current sets the fluctuating axial boundary condition of the plasma and is often called the Bohm Sheath boundary condition. This current condition holds both at the wall and at the sheath entrance. So rather than taking the simulation domain all the way to the wall, simulations often end at the sheath entrance and employ this analytically derived boundary condition to the boundaries of the main plasma. Then one doesn't have to worry about the small spatial scales and the non-quasineutrality of the sheath. The corresponding boundary conditions for the other fluid variables such as the density and temperature have recently been derived by Loizu et al. [LRH12].

The conducting wall mode instability in the case considered here is purely an electron temperature gradient instability, although other types of gradients can cause it [BCR93]. Electron temperature fluctuations are advected by electrostatic potential fluctuations and feed off the equilibrium electron temperature gradient as in the case of the thermal drift waves. However, in contrast to the thermal drift waves, the coupling between the temperature and potential fluctuations comes through the sheath boundary condition rather than through the

adiabatic response.

5.2.2 Bohm Sheath Boundary Implementation

[XRD93]

CHAPTER 6

The Nature of LAPD Turbulence

6.1 A Visual Examination

6.2 A Statistical Examination

CHAPTER 7

Energy Dynamics Formalism

7.1 Total Energy and Dynamics

7.2 Spectral Energy Dynamics

CHAPTER 8

Nonlinear Instability for the Periodic Simulation

8.1 The Energy Spectra

8.2 Energy Dynamics Result

8.3 n=0 Suppression

CHAPTER 9

Energy Dynamics for the Non-periodic Simulations

9.1 The Importance of Axial Boundary Conditions

9.2 Fourier Decomposing Non-periodic Functions

9.3 Energy Dynamics Results

9.4 Linear vs Nonlinear Structure Correlation

CHAPTER 10

Finite Mean Flow Simulations

10.1 The LAPD Biasing Experiment

10.2 New Linear Instabilities

10.3 Statistical Comparisons to Experiment

10.4 Energy Dynamics Results

CHAPTER 11

Conclusion

APPENDIX A

The BOUT++ Code

A.1 The Object-Oriented Fluid Framework

A.2 Explicit Finite Differences

A.3 The Physics Inputs

APPENDIX B

Grid Convergence

References

[BCR93] H. L. Berk, R. H. Cohen, D. D. Ryutov, Yu. A. Tsidulko, and X. Q. Xu. "Electron temperature gradient induced instability induced in tokamak scrape-off layers." *Nuclear Fusion*, **33**:263, 1993.

[Bra65] S. I. Braginskii. "Transport processes in a plasma." In M A Leontovich, editor, *Reviews of Plasma Physics*, volume 1, pp. 205–311. Consultants Bureau, New York, 1965.

[LRH12] J. Loizu, P. Ricci, F. Halpern, and S. Jolliet. "Boundary conditions for plasma fluid models at the magnetic presheath entrance." *Phys. Plasmas*, **13**:122307, 2012.

[PUC10] P. Popovich, M. V. Umansky, T. A. Carter, and B. Friedman. "Analysis of plasma instabilities and verification of BOUT code for linear plasma device." *Phys. Plasmas*, **17**:102107, 2010.

[SC03] A. N. Simakov and P. J. Catto. "Drift-ordered fluid equations for field-aligned modes in low-β collisional plasma with equilibrium pressure pedestals." *Phys. Plasmas*, **10**:4744, 2003.

[Sta00] P. C. Stangeby. *The plasma boundary of magnetic fusion devices*. Institute of Physics Publishing, 2000.

[Wes04] J. Wesson. *Tokamaks*. Clarendon Press, 2004.

[XRD93] X. Q. Xu, M. N. Rosenbluth, and P. H. Diamond. "Electron-temperature-gradient-driven instability in tokamak boundary plasma." *Phys. Fluids B*, **5**:2206, 1993.